

Blue emitting self-assembled nano-crystals of para-sexiphenyl grown by hot wall epitaxy

A. Andreev^{a,c}, F. Quochi^b, H. Sitter^{a,*}, H. Hoppe^c, S. Sariciftci^c, A. Mura^b, G. Bongiovanni^b

^a*Institute of Semiconductor and Solid State Physics, University of Linz, Altenbergerstr., 69, A-4040 Linz, Austria*

^b*Dipartimento di Fisica, Università di Cagliari and Istituto Nazionale per la Fisica della Materia, I-09042 Monserrato (CA), Italy*

^c*Linz Inst. f. Organic Solar Cells (LIOS), Physical Chemistry, University Linz, Altenbergerstr., 69, A-4040 Linz, Austria*

Available online 16 March 2005

Abstract

In this work we report about photoluminescence investigations and the first observation of lasing in highly ordered, crystalline para-sexiphenyl (PSP) films grown by hot wall epitaxy on mica substrates. We demonstrate also the fabrication of hot wall epitaxially grown PSP layers for blue light emitting diodes. The electroluminescence (EL) shows two peaks at 425 and 450 nm, which coincide with the corresponding photoluminescence spectra. The electric field required for the onset of the EL in our single layer devices is comparable with that for optimized multilayer devices based on PSP.

© 2005 Elsevier Ltd. All rights reserved.

Keywords: Self assembling nanostructures; Para-sexiphenyl; Lasing

1. Introduction

Para-sexiphenyl (PSP), a six-units oligomer of poly-paraphenylene, is an attractive material for light-emitting diodes and, potentially, laser diodes due to its high blue electroluminescence efficiency [1], good thermal stability, as well as ability to be purified relatively easy up to electronic grade and to be deposited in form of well ordered films. The latter feature is very important for the fabrication of organic diodes emitting polarized light.

In this work we focus therefore on optical investigations of PSP thin films grown by Hot Wall Epitaxy (HWE). This technique allows to grow epilayers close to thermodynamic equilibrium, which is essential in the case of van der Waals epitaxy of oligomers [2]. In particular, PSP molecules perform a self-organization during growth by HWE on mica substrates resulting in highly ordered blue emitting nano-fibers with dichroic ratios in emission up to 14 [2,3].

2. Experimental

PSP was pre-purified by threefold sublimation under a dynamical vacuum of 1×10^{-6} mbar. Highly ordered, crystalline thin films of PSP have been grown by HWE on freshly cleaved (001)-oriented mica substrates. The vacuum during growth was about 6×10^{-6} mbar. The films were grown at a fixed PSP-source temperature of 240 °C and the substrate temperature was 80 or 130 °C. Further growth details can also be found in Refs. [3,4]. The film morphology was imaged by Atomic Force Microscopy (AFM) using a Dimension 3100 system operated in tapping mode on air.

For lasing experiments the PSP nano-fibers were photoexcited with the frequency-doubled pulses (at 380 nm) of a Ti:Sapphire regenerative amplifier delivering 150-fs-long pulses at 1 kHz repetition rate. A laser spot size of $\approx 120 \mu\text{m}$ (diameter) was used for photoexcitation. The optical emission was collected at different angles with respect to the normal of the substrate, then dispersed in a 46-cm single spectrometer and detected by a cooled charge-coupled device.

The electroluminescence devices were fabricated in a sandwich geometry, using ITO coated glass as bottom and LiF (0.6 nm)/Al (60 nm) as evaporated top electrode. On the ITO, a layer of organic contact material (PEDOT:PSS) was spin coated from an aqueous solution with a thickness of

* Corresponding author. Tel.: +43 732 2468 9623; fax: +43 723 2468 9696.

E-mail address: helmut.sitter@jku.at (H. Sitter).

≈ 100 nm as hole injection layer. After subsequent drying in dynamic vacuum, the active layer of PSP was grown by HWE. EL spectra were measured with an Avantes spectrometer.

3. Results and discussion

Fig. 1 shows an AFM image of the surface morphology of a typical PSP film grown by HWE on mica. The observed long-range ordered structure consists of very long self-assembled nano-fibers, which in turn consist of crystalline domains showing three different epitaxial relationships to the mica substrate [3]. However, the alignment of the PSP long molecular axes is nearly the same in all domains—practically parallel to the substrate and perpendicular to the fiber direction [2,5]. The fibers are parallel to each other and separated by relatively flat areas. A line profile made nearly diagonally (so as to intersect the fibers perpendicularly) shows an average base width and height of the nano-fibers of about 220 and 110 nm, respectively, while the length ranges up to several hundred micrometers. These anisotropic and well-ordered fibers offer a versatile model system for the investigations of linear and non-linear optical properties of nanoscaled organic structures.

Beside steady state photoluminescence (PL) measurements [6], we attempted to achieve laser action in PSP nano-needles. Note, that the last investigations of the nonlinear optical response of oligo-phenylene nano-fibers have shown so far only evidence of spectral narrowing [7]. The sample (its morphology is depicted in Fig. 1) was photoexcited at normal incidence with the laser beam whose polarization was set parallel to the long axis of the PSP molecules, so that a maximum material absorption of $\approx 60\%$ is achieved. Based on the results of recent calculations of the propagation modes for PSP waveguides [8], could be assumed that the PSP emission near 425 nm will propagate with possible amplification only in the (widest) fibers with a width of more than 200–250 nm. Fig. 2 displays a set of time-integrated emission spectra for different values of

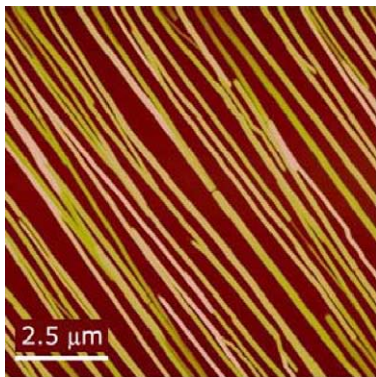


Fig. 1. 10×10 μm topography image of the surface morphology of a PSP film grown by HWE at 130°C on mica.

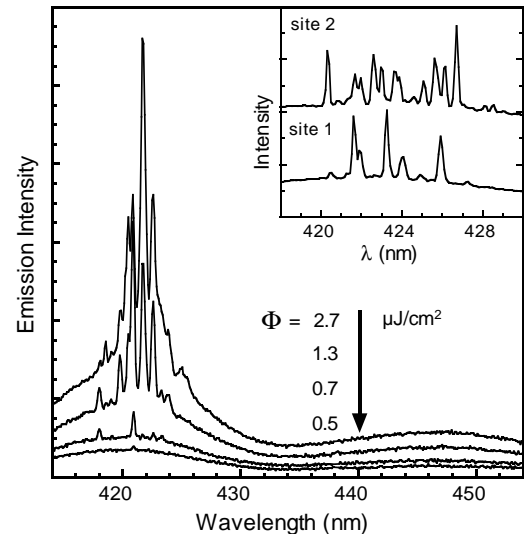


Fig. 2. Emission spectra taken at different values of the pump fluence Φ ($\mu\text{J}/\text{cm}^2$ per pulse). Inset: Emission spectra measured in two different positions across the sample surface at the same excitation level above threshold.

the excitation fluence. The emission is collected nearly perpendicularly to the plane of the mica substrate, but the emission collected at different angles yields similar results. When the pump fluence reaches a given threshold value, very sharp, randomly spaced lines arise at wavelengths across the 0–1 emission band of PSP near 425 nm. Lines having a resolution-limited width (2 \AA) are observed. The line spectral distribution is strongly dependent on the excitation position on the sample surface (insert in Fig. 2). However, the spectral pattern is well reproduced in different acquisitions taken at different times, so that we exclude that the narrow lines are experimental artifacts. The threshold fluence (Φ_{th}) is as low as $0.5 \mu\text{J}/\text{cm}^2$ per pulse (incident on the sample); changes in the sample location yield variations of a factor of three in Φ_{th} . Assuming an internal conversion efficiency of 100%, for $\Phi_{\text{th}} = 0.5 \mu\text{J}/\text{cm}^2$ we estimate a threshold density (N_{th}) of $6 \times 10^{16} \text{ cm}^{-3}$. All the above-mentioned characteristics are found to be independent of temperature in the 30–300 K range; in particular, the threshold fluence remains constant within our 10% experimental accuracy. The observed nonlinear spectra are reminiscent of ‘random lasing’ [9–11]. As the quantity of material deposited between the nano-fibers is negligible, we attribute the optical feedback responsible for laser action to efficient (random) multiple scattering of light propagating along the nano-fibers caused by fiber inhomogeneities. Feedback is possibly provided also by well-defined end facets with good optical quality.

Fig. 3a shows the spectrally-integrated emission intensity as a function of the estimated density (N_0) excited by the ultra fast laser pulses, for densities below threshold. The data actually refer to a position on the sample with a (higher) threshold density $N_{\text{th}} = 2 \times 10^{17} \text{ cm}^{-3}$. The sub-linear dependence of the signal vs N_0 indicates that threshold is

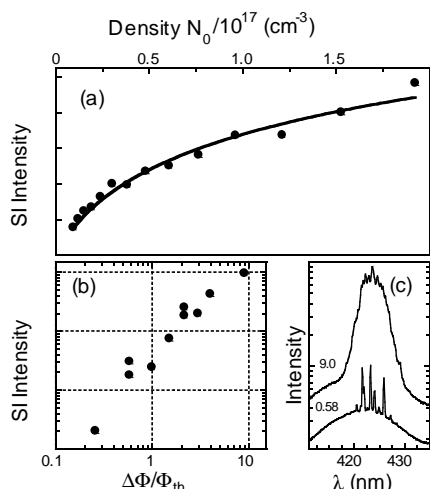


Fig. 3. (a) Spectrally integrated (SI) emission intensity vs photoexcited density N_0 , for pump intensities below threshold. (b) Spectrally integrated pump excess fluence $\Delta\Phi/\Phi_{th}$. (c) Emission spectra recorded at $\Delta\Phi/\Phi_{th} = 0.58$ and 9.0.

achieved in the regime of bimolecular recombination for the photo excited density. For excitation levels just above threshold, laser action first takes place in a few nano-fibers featuring efficient random feedback and long gain paths. Thanks to their narrow linewidth, random modes emerge from the intense spontaneous emission spectrum resulting from all the other fibers, which are characterized by higher optical losses. These latter represent the majority of the crystalline needles. As one would expect, the evolution of the emission spectrum as a function of the excitation power is very similar to that reported in an ensemble of dye-filled micro crystals, where laser oscillation begins on a single crystal, while all the other microresonators, supporting lossier modes, contribute to the ensemble response with spontaneous emission only [12]. The emission intensity for excitation levels above Φ_{th} is plotted in Fig. 3b as a function of the normalized pump excess fluence, defined as $\Delta\Phi/\Phi_{th} \equiv (\Phi - \Phi_{th})/\Phi_{th}$. The signal is spectrally integrated over the random lasing spectrum, after subtraction of the spontaneous emission contribution. The emission varies superlinearly with $\Delta\Phi/\Phi_{th}$. At small values of $\Delta\Phi/\Phi_{th}$, the number of oscillating modes increases with increasing pump fluence, since different random modes are characterized by different lasing thresholds [11]; as a consequence, the total emission of the narrow lines increases superlinearly with increasing $\Delta\Phi/\Phi_{th}$. Eventually, amplified spontaneous emission (ASE) is achieved along nano-fibers with higher optical losses and not contributing to lasing. The rise of an ASE band explains (i) the persistence of the superlinear growth of the emission intensity [10] and (ii) the progressive decrease in visibility of the random lasing modes at large values of $\Delta\Phi/\Phi_{th}$, as shown in Fig. 3c.

Unfortunately, light-emitting or laser diodes cannot be realizable on mica, which is a strong insulator.

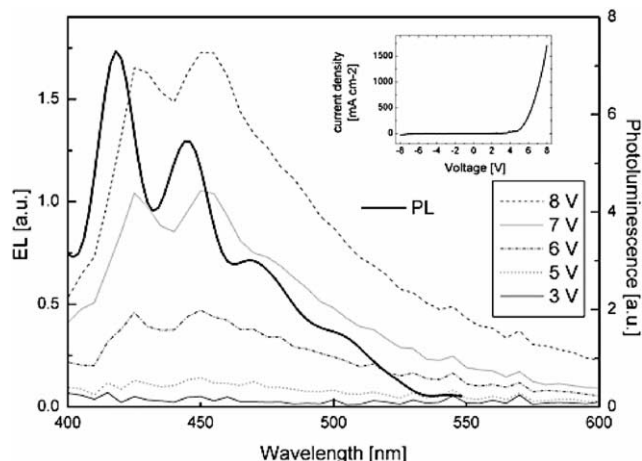


Fig. 4. Electroluminescence of a PSP ($d = 100 \text{ nm}$) single device at different voltage. Inset shows the corresponding current–voltage curve. Full line shows the photoluminescence of a PSP film on mica.

So, as the first attempt we tested HWE grown PSP layers for electroluminescence (EL) using ITO/PEDOT/PSP/LiF/Al structures. Fig. 4 shows the typical EL spectra obtained. Corresponding I – V curves show a rectification value of ~ 100 at $\pm 7 \text{ V}$ and an onset for the current injection at $+ 5 \text{ V}$. The EL shows two peaks at 425 and 450 nm. The onset for EL is between 5 and 6 V and coincides with the onset of current injection. The PL spectrum of PSP shows similar features as the EL, but is shifted for $\approx 10 \text{ nm}$ to the blue. These observations are in a good agreement with literature data [1,13]. It is worth to mention here that the electrical field ($\approx 5 \times 10^5 \text{ V/cm}$) required for the onset of the EL in our single layer devices is comparable with that for optimised multilayer devices based on PSP [13].

4. Conclusion

In summary, we present the results of optical investigations on PSP thin films grown by HWE. We report the first experimental evidence of random laser action in HWE grown PSP nano-fibers. Threshold fluences as low as $0.5 \mu\text{J/cm}^2$ are observed with subpicosecond pulses as the excitation source. On the other hand, PSP single layer devices grown using HWE on ITO/PEDOT substrates display blue electroluminescence, which shows a spectrum comparable with photoluminescence.

Acknowledgements

We acknowledge the financial support from the Austrian Foundation for Advancement of Scientific Research (FWF projects P-15155, P-15627, P-15629 and P-15630-N08) and partial support from the EC RTN ‘Nanochannels’ (contract no. HPRN-CT-2002-00323). Part of this work was performed within the Christian Doppler Society’s dedicated

laboratory on Plastic Solar Cells funded by the Austrian Ministry of Economic Affairs and Konarka Austria Ges.m.b.H.

References

- [1] H. Yanagi, S. Okamoto, *Appl. Phys. Lett.* 71 (1997) 2563; S. Tasch, C. Brandstätter, F. Meghdadi, G. Leising, G. Froyer, L. Athouel, *Adv. Mater.* 9 (1997) 33.
- [2] A. Andreev, G. Matt, C.J. Brabec, H. Sitter, D. Badt, H. Seyringer, N.S. Sariciftci, *Adv. Mater.* 12 (2000) 629.
- [3] H. Plank, R. Resel, S. Purger, J. Keckes, A. Thierry, B. Lotz, A. Andreev, N.S. Sariciftci, H. Sitter, *Phys. Rev. B* 64 (2001) 235423.
- [4] H. Plank, R. Resel, A. Andreev, N.S. Sariciftci, H. Sitter, *J. Cryst. Growth* 237–239 (2002) 2076.
- [5] H. Plank, R. Resel, H. Sitter, A. Andreev, N.S. Sariciftci, G. Hlawacek, C. Teichert, A. Thierry, B. Lotz, *Thin Solid Films* 443 (2003) 108.
- [6] A. Kadashchuk, A. Andreev, H. Sitter, S. Sariciftci, *Synth. Met.* 139 (2003) 937–940.
- [7] H. Yanagi, T. Ohara, T. Morikawa, *Adv. Mater.* 13 (2001) 1452.
- [8] F. Balzer, V.G. Bordo, A.C. Simonsen, H.-G. Rubahn, *Phys. Rev. B* 67 (2003) 115408.
- [9] S.V. Frolov, Z.V. Vardeny, K. Yoshino, A. Zakhidov, R.H. Baughman, *Phys. Rev. B* 59 (1999) R5284.
- [10] M. Anni, S. Lattante, R. Cingolani, G. Gigli, G. Barbarella, L. Favaretto, *Appl. Phys. Lett.* 83 (2003) 2754.
- [11] H. Cao, Y.G. Zhao, S.T. Ho, E.W. Seelig, Q.H. Wang, R.P.H. Chang, *Phys. Rev. Lett.* 82 (1999) 2278.
- [12] G. Ihlein, F. Schüth, O. Krauß, U. Vietze, F. Laeri, *Adv. Mater.* 10 (1998) 1117.
- [13] F. Meghdadi, S. Tasch, B. Winkler, W. Fischer, F. Stelzer, G. Leising, *Synth. Met.* 85 (1997) 1441.